Acta Crystallographica Section D
Biological Crystallography
ISSN 0907-4449

The structure of brazzein, a sweet-tasting protein from the wild African plant *Pentadiplandra brazzeana*

Koji Nagata,[a] Nobuko Hongo,[a] Yasuhiro Kameda,[a] Akihiro Yamamura,[a] Hiroshi Sasaki,[a] Woo Cheol Lee,[a] Kohki Ishikawa,[b] Ei-ichiro Suzuki[b] and Masaru Tanokura[a]*

[a]Department of Applied Biological Chemistry, Graduate School of Agricultural and Life Sciences, The University of Tokyo, 1-1-1 Yayoi, Bunkyo-ku, Tokyo 113-8657, Japan, and [b]Institute for Innovation, Ajinomoto Co. Inc., Suzuki-cho, Kawasaki-ku, Kawasaki-shi, Kanagawa 210-8681, Japan

Correspondence e-mail: amtanok@mail.ecc.u-tokyo.ac.jp

Received 30 October 2012
Accepted 10 January 2013

PDB Reference: brazzein, 4he7

Brazzein is the smallest sweet-tasting protein and was isolated from the wild African plant *Pentadiplandra brazzeana*. The brazzein molecule consists of 54 amino-acid residues and four disulfide bonds. Here, the first crystal structure of brazzein is reported at 1.8 Å resolution and is compared with previously reported solution structures. Despite the overall structural similarity, there are several remarkable differences between the crystal and solution structures both in their backbone folds and side-chain conformations. Firstly, there is an additional α-helix in the crystal structure. Secondly, the atomic r.m.s.d.s between the corresponding C^{α}-atom pairs are as large as 2.0–2.2 Å between the crystal and solution structures. Thirdly, the crystal structure exhibits a molecular shape that is similar but not identical to the solution structures. The crystal structure of brazzein reported here will provide additional information and further insights into the intermolecular interaction of brazzein with the sweet-taste receptor.

1. Introduction

Several proteins have been reported to act as sweeteners: brazzein (Ming & Hellekant, 1994; Kohmura *et al.*, 1996), thaumatin (van der Wel & Loeve, 1972; Iyengar *et al.*, 1979), monellin (Morris & Cagan, 1972; van der Wel, 1972; Frank & Zuber, 1976), curculin (Yamashita *et al.*, 1990; Shirasuka *et al.*, 2004; Suzuki *et al.*, 2004; Kurimoto *et al.*, 2007), mabinlin (Liu *et al.*, 1993) and pentadin (van der Wel *et al.*, 1989). Brazzein, a 6.5 kDa protein consisting of 54 amino acids and four disulfide bonds, is the smallest sweet-tasting protein yet isolated and was obtained from the wild African plant *Pentadiplandra brazzeana*. Brazzein has various desirable properties for use as a low-calorie sweetener in the diets of individuals suffering from diabetes, obesity and metabolic syndrome. For example, brazzein has a high water solubility of greater than 50 mg ml^{-1} and a high thermostability such that its sweetness remains even after incubation at 353 K for 4 h (Ming & Hellekant, 1994). In addition, brazzein is 2000 times sweeter than sucrose on a weight basis and has a more phasic response and a faster adapting tonic phase than thaumatin (Ming & Hellekant, 1994).

Mammals taste many compounds, yet they use a sensory palette consisting of only five basic tastes: sweet, bitter, sour, salty and umami. The molecular mechanisms of taste sensing have been revealed based on these five basic tastes (Huang *et al.*, 2006). Two families of taste receptors, T1Rs and T2Rs, are involved in sensing sweet, umami and bitter tastes. T1Rs are a small family of three G-protein-coupled receptors (GPCRs) that are expressed in taste cells on the tongue and palate epithelium. The T1R members form two heterodimeric receptors. The T1R1–T1R3 heterodimer functions as the

umami sensor that recognizes L-glutamate and most of the other L-amino acids, while the T1R2–T1R3 heterodimer functions as a broadly tuned sweet sensor that recognizes all of the sweeteners tested, including sugars, D-amino acids, sweet proteins and various artificial sweeteners (Zhao *et al.*, 2003). However, the potential sites of interaction between the various sweet proteins and the T1R2–T1R3 receptor vary. Monellin and thaumatin have been proposed to bind to the Venus flytrap module (VFTM) of T1R2 (Temussi, 2002), brazzein to the cysteine-rich domain (CRD) of T1R3 (Jiang *et al.*, 2004) and curculin (neoculin) to the VFTM of T1R3 (Shimizu-Ibuka *et al.*, 2006).

The solution structure of brazzein determined by ^{1}H NMR spectroscopy at pH 5.2 and 295 K (PDB entries 1brz and 2brz; Caldwell *et al.*, 1998) shows that brazzein contains one short α-helix (residues 21–29) and an antiparallel β-sheet consisting of three β-strands (residues 5–7, 34–39 and 44–50). Interestingly, both the secondary structure derived from the NOE data of brazzein at pH 3.5 and 300 K (Gao *et al.*, 1999) and the solution structure of des-pGlu1-brazzein, which lacks the N-terminal pyroglutamate (pGlu), at pH 5.2 and 310 K (PDB entry 2kgq; Center for Eukaryotic Structural Genomics, unpublished work) indicate that residues 14–17 form a 3_{10}-helix which is not observed in the abovementioned solution structure of full-length brazzein at pH 5.2 and 295 K. The critical regions for eliciting the sweetness of brazzein have been localized into three sites: site 1 (loop 43), site 2 (the N- and C-termini and the adjacent Glu36; loop 33) and site 3 (loop 9–19) (Assadi-Porter *et al.*, 2010). Mutagenic analysis of the sweet-taste receptor T1R2–T1R3 indicates that the residue Ala537 in the CRD of T1R3 plays an essential role in activation of the receptor by brazzein binding (Jiang *et al.*, 2004). However, the molecular mechanism of the activation of T1R2–T1R3 by brazzein binding is still obscure.

Here, we report the first crystal structure of brazzein, at 1.8 Å resolution, and compare it with the reported solution structures. Some remarkable differences have been found between the crystal and solution structures of brazzein.

2. Materials and methods

2.1. Structure solution and refinement

The purification, crystallization and X-ray diffraction data collection of brazzein have been reported previously (Ishikawa *et al.*, 1996). In brief, crystals of native brazzein, consisting of full-length brazzein and des-pGlu1-brazzein as the major and minor forms, respectively, were obtained by the hanging-drop vapour-diffusion method, with the hanging drop being established by mixing an equal volume of 10–15 mg ml^{-1} protein solution with 0.9–1.0 *M* sodium citrate pH 4.0 and being equilibrated against a reservoir containing the same concentration of sodium citrate pH 4.0 at 293 K. X-ray diffraction data were collected from the brazzein crystal to 1.8 Å resolution on BL-6A at the Photon Factory, Ibaraki, Japan. The crystal belonged to space group $I4_122$, with unit-cell parameters $a = b = 61.4$, $c = 59.6$ Å.

Table 1
Refinement statistics.

Values in parentheses are for the highest resolution shell.

Resolution range (Å)	42.8–1.80 (1.847–1.800)
Completeness (%)	92.9 (83.1)
No. of reflections used in refinement	4890 (309)
R† (%)	21.9 (37.6)
R_{free}‡ (%)	25.2 (41.3)
Average B (Å^2)	21.6
No. of protein residues modelled	54
No. of protein atoms modelled	449
No. of water molecules modelled	13
No. of sodium ions modelled	0.5
R.m.s.d. from ideal values, bond lengths (Å)	0.018
R.m.s.d. from ideal values, bond angles (°)	2.124
Ramachandran plot (%)	
Residues in favoured regions	94.1
Residues in additionally allowed regions	5.9
Residues in outlier regions	0

† $R = \sum_{hkl} \sum_i |I_i(hkl) - \langle I(hkl)\rangle| / \sum_{hkl} \sum_i I_i(hkl)$, where F_{obs} and F_{calc} are the observed and calculated structure-factor amplitudes for reflection hkl, respectively. ‡ R_{free} is calculated using 5% of the reflections, which were randomly excluded from all the stages of refinement.

Molecular replacement was performed with the program *MOLREP* (Vagin & Teplyakov, 2010) in the single-model (best solution of averaged RF and individual TFs) mode using the solution structure of brazzein (PDB entry 2brz; Caldwell *et al.*, 1998) as a molecular model. The obtained structural model was iteratively refined using *Coot* (Emsley & Cowtan, 2004) and *REFMAC* (Murshudov *et al.*, 2011). The final refinement using *REFMAC* consisted of ten steps of TLS (translation/libration/screw) refinement (Winn *et al.*, 2003) followed by ten steps of restrained refinement. The abovementioned programs are included in the *CCP*4 suite (Winn *et al.*, 2011). The TLS tensors were obtained with *TLSMD* (Painter & Merritt, 2006). The stereochemistry of the structure was checked using the program *RAMPAGE* (Lovell *et al.*, 2003).

2.2. Structure analyses

Superimpositions of structures and calculations of atomic r.m.s.d.s were performed with *LSQKAB* (Kabsch, 1976) in the *CCP*4 suite. The secondary-structure elements were assigned with *STRIDE* (Heinig & Frishman, 2004). The molecular assembly in the crystal was analyzed using *PISA* (Krissinel & Henrick, 2007). The molecular graphics were prepared with *PyMOL* (DeLano, 2002) and *Coot*.

2.3. Gel-filtration analysis

Gel-filtration analysis of brazzein was performed using a Superdex 75 10/300 GL column (GE Healthcare) and an elution buffer consisting of 25 m*M* HEPES–NaOH pH 7.5 and 0, 100, 200 or 500 m*M* NaCl at a flow rate of 0.5 ml min^{-1} at 298 K. 100 µl brazzein solution (10 mg ml^{-1}) dissolved in elution buffer containing 0, 100, 200 or 500 m*M* NaCl was injected in each run. The elution volume of brazzein in each elution buffer was compared with those of ribonuclease A (13.7 kDa) and aprotinin (6.5 kDa) in elution buffer containing 150 m*M* NaCl.

3. Results and discussion

3.1. Crystal structure of brazzein

We solved the crystal structure of brazzein by the molecular-replacement method using the diffraction data at 1.8 Å resolution (Ishikawa *et al.*, 1996) with the solution structure of brazzein (PDB entry 2brz; Caldwell *et al.*, 1998) as a molecular model. The refinement statistics are summarized in Table 1. The final structure consists of one brazzein molecule (residues 1–54), one sodium ion and 13 water molecules in the asymmetric unit (Fig. 1). The main-chain and side-chain atoms of all of the amino-acid residues except for the side chains of Asp2, Lys3, Lys6 and Lys42 were well placed in the electron density, with no breaks in the $2F_o - F_c$ map contoured at 1σ. Eight cysteine residues form four intramolecular disulfide bonds, Cys4–Cys52, Cys16–Cys37, Cys22–Cys47 and Cys26–Cys49, which is consistent with the previous report (Kohmura *et al.*, 1996). The crystal structure of brazzein contains secondary-structure elements similar to those in the solution structure: one short α-helix (α2, residues 21–30) and three β-strands (β1, residues 4–6; β2, residues 34–39; β3, residues 45–50), which form a triple-stranded antiparallel β-sheet (Fig. 1*a*). The crystal structure also contains an additional α-helix (α1) at residues 13–17 which is not observed in the solution structure.

Brazzein exists as a monomer in solution. However, it forms a homodimer in the crystal, probably owing to crystal-packing effects (Fig. 1*b*). The dimer interface of brazzein accounts for 11% (860 Å^2) of the total surface area of the homodimer (7760 Å^2). The free energy of assembly dissociation for the brazzein dimer (4.3 kcal mol^{-1}) suggests that the two brazzein protomers in the dimer are weakly associated. In fact, no dimerization of brazzein has been observed in solution even at 50 mg ml^{-1} (Caldwell *et al.*, 1998) or at 10 mg ml^{-1} in 0–500 m*M* NaCl (this study). The dimeric brazzein is stabilized by six hydrogen bonds: Gln17 O···Ala19′ N, Ala19 N···Gln17′ O, Asn20 N$^{\delta2}$···Cys37′ O, Cys37 O···Asn20′ N$^{\delta2}$, Tyr24 O$^{\eta}$···Glu36′ O$^{\varepsilon2}$ and Glu36 O$^{\varepsilon2}$···Tyr24′ O$^{\eta}$ (where a prime indicates that the residue is in an adjacent brazzein molecule in the crystal). In addition, a sodium ion, which came from the reservoir solution, which contained 0.9–1.0 *M* sodium citrate pH 4.0, is observed at the dimer interface. Two protein atoms (Asn20 N and Asn20′ N) and four water molecules are coordinated to the sodium ion (Fig. 1*c*). Part (Cys16-Gln17) of the additional α-helix (α1, residues 13–17) is involved in the dimer interface. This implies that α-helix α1 may be stabilized by formation of the homodimer. Since the sodium ion is observed in the dimer interface, we performed gel-filtration analysis of brazzein at different NaCl concentrations in the elution buffer. Homodimerization of brazzein did not occur at a protein concentration of 10 mg ml^{-1} even at the high salt concentration of 500 m*M* NaCl at pH 7.5 (data not shown).

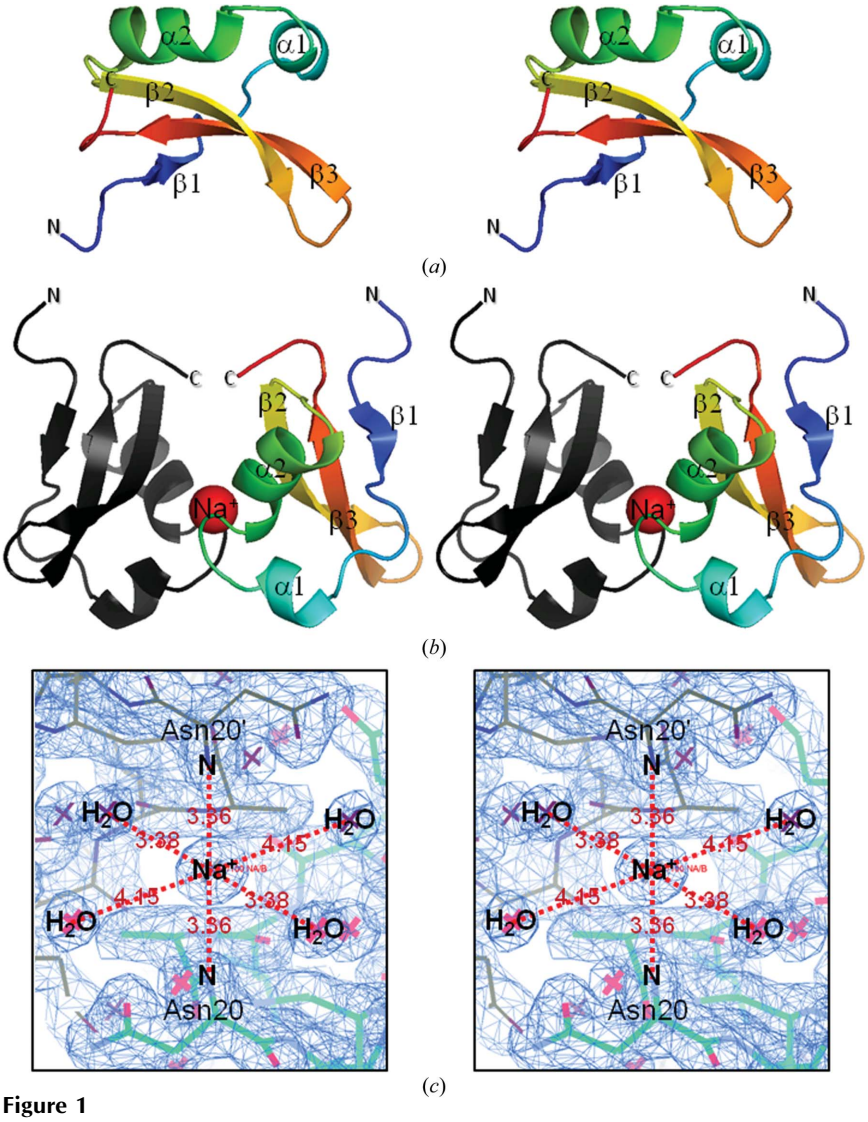

Figure 1
Stereoview of the overall structure of brazzein. The N- and C-termini as well as the secondary-structure elements β-strands (β1–3) and α-helices (α1–2) are labelled. (*a*) Structure of a brazzein monomer. (*b*) Structure of a brazzein homodimer. One protomer is coloured as in (*a*), while the other protomer is coloured black. The sodium ion between the protomers is shown as a red sphere. (*c*) The coordination of the sodium ion. Interatomic distances (Å) are shown in red.

3.2. Comparison of the crystal structure of brazzein with the NMR structures

The overall folds of the crystal and solution structures of brazzein (PDB entry 2brz; Caldwell *et al.*, 1998) are apparently similar, but the r.m.s.d. for the 54 pairs of C$^{\alpha}$ atoms is as high as 2.0 Å. The r.m.s.d. for C$^{\alpha}$ atoms among 43 members of the NMR ensemble (PDB entry 1brz; Caldwell *et al.*, 1998) is 2.3 Å, indicating that the solution structure of brazzein obtained by two-dimensional

^{1}H NMR is not well converged. Recently, another solution structure of brazzein (specifically, des-pGlu1-brazzein) has been deposited (PDB entry 2kgq; Center for Eukaryotic Structural Genomics, unpublished work). Although this solution structure, which was obtained by two- and three-dimensional heteronuclear NMR using ^{15}N- and ^{13}C,^{15}N-labelled proteins, is well determined to an r.m.s.d. of 0.8 Å for C^{α} atoms among the 20 members of the NMR ensemble, the r.m.s.d. between the crystal structure of brazzein and this solution structure is 2.2 Å for 53 pairs of C^{α} atoms (excluding pGlu1), indicating the essential difference between the crystal structure and this solution structure. The largest structural differences between the crystal structure and these solution structures are found in the loop regions and the terminal regions (Fig. 2). Interestingly, the solution structures of brazzein (PDB entries 2brz) and des-pGlu1-brazzein (PDB entry 2kgq) are also essentially different from each other, with an r.m.s.d. of 2.1 Å for 53 pairs of C^{α} atoms. The structural differences among the crystal and the two solution structures probably result from intrinsic structural differences among the three conditions with different states (crystalline *versus* solution), pH values, temperatures and buffer compositions. The protein structure in the crystal should be less mobile and could be fixed in fewer or a single conformation(s) owing to crystal-packing effects. In the crystal structure of brazzein, dimerization could cause deformation of the brazzein protomer, particularly at the dimer interface. The protein structure in solution should be more flexible than the crystal structure, and the conformational restraints derived from the solution NMR data could be insufficient and/or less accurate. Interestingly, α-helix α1 (residues 13–17), which is uniquely found in the crystal structure of brazzein obtained at pH 4.0 and 293 K, is formed in the region corresponding to that where a 3_{10}-helix is formed in the solution structure of des-pGlu1-brazzein obtained at pH 5.2 and 310 K (residues 14–17; PDB entry 2kgq; Center for Eukaryotic Structural Genomics, unpublished work) and a 3_{10}-helix is predicted to be formed based on the NOE data of brazzein obtained at pH 3.5 and 300 K (residues 14–17; Gao *et al.*, 1999). In contrast, the corresponding region in the solution structure of brazzein obtained at pH 5.2 and 295 K (PDB entry 2brz) adopts a loop structure instead of an α-helix or a 3_{10}-helix (Caldwell *et al.*, 1998). Thus, the α1 helix should be less stable than the α2 helix, with a probable conformational equilibrium in this region in solution: loop$\leftrightarrow 3_{10}$-helix$\leftrightarrow\alpha$-helix. The α1 helix could be stabilized by crystal-packing effects.

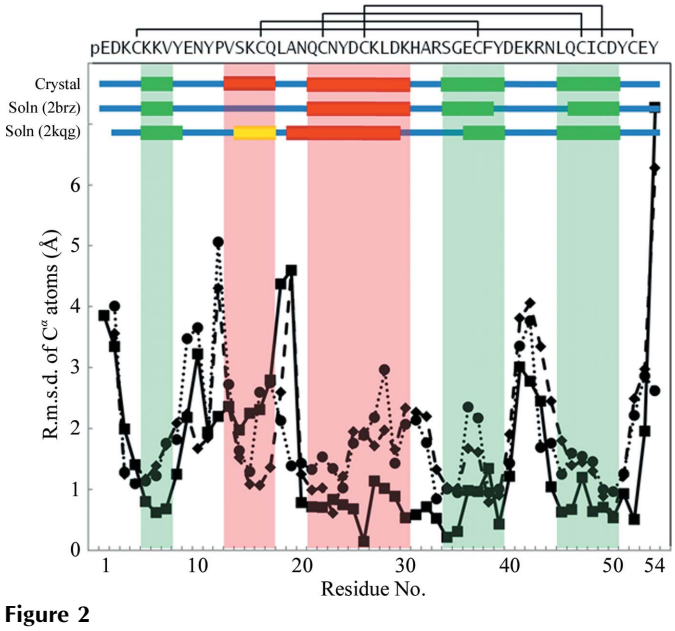

Figure 2
Comparison of the crystal structure and solution structures of brazzein. The r.m.s.d. of the C^{α} atom of each residue is plotted. The continuous, dashed and dotted lines indicate comparisons of the crystal structure *versus* the solution structure (PDB entry 2brz), the crystal structure *versus* the solution structure (PDB entry 2kqg) and the solution structure (PDB entry 2brz) *versus* the solution structure (PDB entry 2kqg), respectively. In the secondary-structure representation, α-helices, 3_{10}-helices and β-strands, as assigned by *STRIDE* (Heinig & Frishman, 2004), are shown as red, yellow and green bars, respectively. The α-helix and β-strand regions in the crystal structure are coloured pink and light green, respectively.

3.3. Distribution of important residues for the sweetness of brazzein

Various deletion, insertion and point mutants of brazzein have been prepared and their sweet-tasting activities have been evaluated (Assadi-Porter *et al.*, 2000, 2010; Jin *et al.*, 2003; Walters *et al.*, 2009; Yoon *et al.*, 2011; Do *et al.*, 2011). The importance of each amino-acid residue for the sweet-tasting activity was re-evaluated using the published activity data for the point mutants of brazzein (Supplementary Tables S1 and S2[1]), but not the data for insertion or deletion mutants, because such insertions or deletions could affect the main-chain fold and the side-chain conformations of other residues. The data for des-pGlu1-brazzein (Assadi-Porter *et al.*, 2000) were used as a sole exception because pGlu1 does not interact with any other residues in either the crystal or the solution structure and thus deletion of pGlu1 would not affect the conformation of the other part. Important side chains were identified by the activities of Ala mutants, while important characteristics of the side chains were identified by the activities of other point mutants. If a point mutation to Ala made the mutant non-sweet, less sweet, sweeter or equally sweet, this side chain was considered to be 'critical', 'important', 'involved' or 'not important' (coloured blue, light blue, red and grey in Fig. 3), respectively, for the sweet-tasting activity. In Fig. 3, the residues coloured beige are residues for which mutational data have not been reported, while residues coloured green are those for which point mutants other than the Ala mutant indicate that the residues somehow contribute to the sweetness of brazzein. The eight Cys residues which form four disulfide bonds are coloured orange.

A total of 16 residues have been mutated to Ala and are grouped into five critical (Lys30, Arg33, Glu36, Tyr39 and Arg43), seven important (Lys5, Lys6, Tyr8, Lys15, His31,

[1] Supplementary material has been deposited in the IUCr electronic archive (Reference: MH5080). Services for accessing this material are described at the back of the journal.

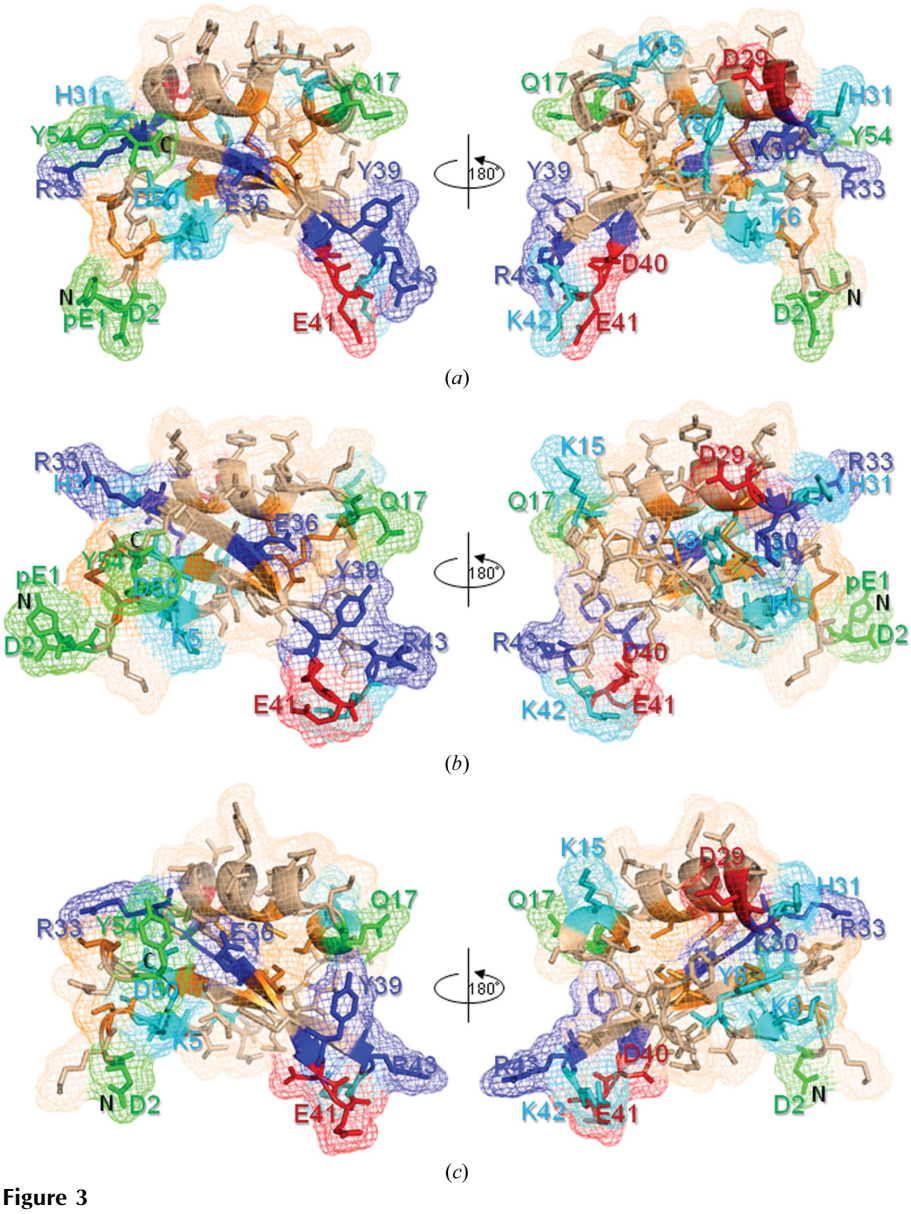

Figure 3
The residues important for the sweetness of brazzein. The molecular surfaces of (*a*) the crystal structure, (*b*) the solution structure (PDB entry 2brz) and (*c*) the solution structure (PDB entry 2kqg) are shown. The left and right panels show front and back views, respectively. The amino-acid residues coloured blue, light blue, red and grey are the 'critical', 'important', 'involved' and 'not important' residues, respectively, as judged based on the activities of the Ala mutants. Residues coloured beige are residues for which mutational data have not been reported, while residues coloured green are residues for which point mutants other than the Ala mutant indicate that the residues contribute to the sweetness of brazzein. The eight Cys residues which form four disulfide bonds are coloured orange.

Lys42 and Asp50) and four involved (Gln17, Asp29, Asp40 and Glu41) residues (Supplementary Tables S1 and S2). Other point mutations and the deletion of pGlu1 indicate that pGlu1, Asp2 and Tyr54 at the N- and C-termini are also involved in the sweet-tasting activity of brazzein. The mutagenic analyses indicate that the residues important for the sweet-tasting activity are widespread on the molecular surface of brazzein (Fig. 3). Of the five critical residues, Lys30 and Glu36 are located on the opposite side of the molecule to Arg33 and Tyr39/Arg43, with all of the side chains highly exposed to the solvent, suggesting multiple-site interactions between brazzein and the sweet-taste receptor. It has been proposed that there are three active sites on the molecular surface of brazzein based on the mutagenesis data and the solution structure (Assadi-Porter *et al.*, 2010). These proposed active sites 1–3 are also observed in the crystal structure. However, the proposed active sites exhibit different shapes and characteristics between the crystal and solution structures owing to their different main-chain and side-chain conformations (Fig. 3).

3.3.1. Site 1. This site consists of Tyr39, Asp40, Glu41, Lys42 and Arg43, which are located on the type I β-turn between the β2 and β3 strands. The two critical residues, Arg43 and Tyr39, form a cation–π interaction between the backbone amide group of Arg43 and the phenyl group of Tyr39. The side chain of Arg42 forms an electrostatic interaction with the side chain of Glu41. These inter-residue interactions stabilize the characteristic conformation of the critical and important side chains of Tyr39, Lys42 and Arg43 as well as the involved side chains of Asp40 and Glu41.

3.3.2. Site 2. This site consists of the N- and C-termini as well as the central part of the molecule (pGlu1, Asp2, Lys5, Lys6, Tyr8, His31, Lys42, Asp50 and Tyr54). The three critical side chains in this site, Lys30, Arg33 and Glu36, are located separately. The side chain of Glu36 is fully exposed to the solvent, indicating that this side chain is directly involved in receptor recognition. The side chain of Lys30 is located on the opposite side of the molecule and forms a cation–π interaction with the important side chain of Tyr8 to stabilize the relative arrangement of the α2 helix and the loop between the β1 strand and the α1 helix. Since the Lys30Arg mutation significantly lowers the sweetness of brazzein (Yoon *et al.*, 2011), the side chain of Lys30 itself and/or the molecular surface stabilized by the cation–π interaction between Lys30 and Tyr8 are/is very important for the sweet-taste activity. The side chain of Arg33 interacts with the side chain of Tyr54 by a cation–π interaction and with the backbone carbonyl group of Cys52 by a hydrogen bond. These interactions help to stabilize the relative arrangement of the β1 strand and the C-terminal part. The side chain of Lys5 forms electrostatic interactions with the side chains of Asp50 and Glu36 and contributes to the stabilization of the antiparallel β-sheet formed by the β1 and

β3 strands. The side chain of Lys6 is exposed to solvent without interacting with any other side chains, suggesting its importance in receptor binding. The N-terminal residues pGlu1 and Asp2 must be involved in receptor recognition as des-pGlu1-brazzein (Assadi-Porter *et al.*, 2000) is twice as sweet as the wild type (Assadi-Porter *et al.*, 2000) and the Asp2Glu mutant is sweeter than the wild type (Assadi-Porter *et al.*, 2010). As mentioned above, there are many interactions between the terminal and central parts of brazzein in site 2 and these contribute to the stabilization of the active conformation of brazzein.

3.3.3. Site 3. This site has also been referred to as loop 9–19 (Assadi-Porter *et al.*, 2010). However, only the side chains of Lys15 and Gln17 are shown to be important and involved, respectively, by point mutations. The side chain of Lys15 forms electrostatic interactions with the side chains of Gln21 and Asp24. The side chain of Gln17 is fully exposed to the solvent. Since the Gln17Asn mutant showed significantly reduced sweet-tasting activity (Yoon *et al.*, 2011), the side chain of Gln17 should be involved in receptor recognition, although the Gln17Ala mutant retains a sweet-tasting activity equivalent to that of wild-type brazzein (Assadi-Porter *et al.*, 2000; Jin *et al.*, 2003). The site 3 residues Lys15 and Gln17 are located on the α1 helix in the crystal structure. Because this region can adopt multiple main-chain conformations such as a loop, a 3_{10}-helix and an α-helix, the conformational state of this site can have an effect on the sweet-tasting activity of brazzein.

Models of the binding between brazzein and the T1R2–T1R3 sweet-taste receptor have been built using the solution structure. The crystal structure of brazzein will provide additional information and further insights into the manner of receptor recognition of brazzein.

The synchrotron-radiation experiments were performed at Photon Factory BL-6A, Tsukuba, Japan under the approval of the Photon Factory Program Advisory Committee (Proposal Nos. 1996F192 and 2000G306). This work was partly supported by Grants-in-Aid for Scientific Research from the Ministry of Education, Culture, Sports, Science and Technology of Japan and by the Targeted Proteins Research Program (TPRP) of the Ministry of Education, Culture, Sports, Science and Technology of Japan.

References

Assadi-Porter, F. M., Aceti, D. J. & Markley, J. L. (2000). *Arch. Biochem. Biophys.* **376**, 259–265.
Assadi-Porter, F. M., Maillet, E. L., Radek, J. T., Quijada, J., Markley, J. L. & Max, M. (2010). *J. Mol. Biol.* **398**, 584–599.
Caldwell, J. E., Abildgaard, F., Dzakula, Z., Ming, D., Hellekant, G. & Markley, J. L. (1998). *Nature Struct. Biol.* **5**, 427–431.
DeLano, W. L. (2002). *CCP4 Newsl. Protein Crystallogr.* **40**, contribution 11.
Do, H., Jo, H., Jo, D. & Kong, K. (2011). *Bull. Korean Chem. Soc.* **32**, 4106–4108.
Emsley, P. & Cowtan, K. (2004). *Acta Cryst.* D**60**, 2126–2132.
Frank, G. & Zuber, H. (1976). *Hoppe Seylers Z. Physiol. Chem.* **357**, 585–592.
Gao, G.-H., Dai, J.-X., Ding, M., Hellekant, G., Wang, J.-F. & Wang, D.-C. (1999). *Int. J. Biol. Macromol.* **24**, 351–359.
Heinig, M. & Frishman, D. (2004). *Nucleic Acids Res.* **32**, W500–W502.
Huang, A. L., Chen, X., Hoon, M. A., Chandrashekar, J., Guo, W., Tränkner, D., Ryba, N. J. P. & Zuker, C. S. (2006). *Nature (London)*, **442**, 934–938.
Ishikawa, K., Ota, M., Ariyoshi, Y., Sasaki, H., Tanokura, M., Ming, D., Caldwell, J. & Abilgaad, F. (1996). *Acta Cryst.* D**52**, 577–578.
Iyengar, R. B., Smits, P., van der Ouderaa, F., van der Wel, H., van Brouwershaven, J., Ravestein, P., Richters, G. & van Wassenaar, P. D. (1979). *Eur. J. Biochem.* **96**, 193–204.
Jiang, P., Ji, Q., Liu, Z., Snyder, L. A., Benard, L. M., Margolskee, R. F. & Max, M. (2004). *J. Biol. Chem.* **279**, 45068–45075.
Jin, Z., Danilova, V., Assadi-Porter, F. M., Aceti, D. J., Markley, J. L. & Hellekant, G. (2003). *FEBS Lett.* **544**, 33–37.
Kabsch, W. (1976). *Acta Cryst.* A**32**, 922–923.
Kohmura, M., Ota, M., Izawa, H., Ming, D., Hellekant, G. & Ariyoshi, Y. (1996). *Biopolymers*, **38**, 553–556.
Krissinel, E. & Henrick, K. (2007). *J. Mol. Biol.* **372**, 774–797.
Kurimoto, E., Suzuki, M., Amemiya, E., Yamaguchi, Y., Nirasawa, S., Shimba, N., Xu, N., Kashiwagi, T., Kawai, M., Suzuki, E. & Kato, K. (2007). *J. Biol. Chem.* **282**, 33252–33256.
Liu, X., Maeda, S., Hu, Z., Aiuchi, T., Nakaya, K. & Kurihara, Y. (1993). *Eur. J. Biochem.* **211**, 281–287.
Lovell, S. C., Davis, I. W., Arendall, W. B., de Bakker, P. I., Word, J. M., Prisant, M. G., Richardson, J. S. & Richardson, D. C. (2003). *Proteins*, **50**, 437–450.
Ming, D. & Hellekant, G. (1994). *FEBS Lett.* **355**, 106–108.
Morris, J. A. & Cagan, R. H. (1972). *Biochim. Biophys. Acta*, **261**, 114–122.
Murshudov, G. N., Skubák, P., Lebedev, A. A., Pannu, N. S., Steiner, R. A., Nicholls, R. A., Winn, M. D., Long, F. & Vagin, A. A. (2011). *Acta Cryst.* D**67**, 355–367.
Painter, J. & Merritt, E. A. (2006). *J. Appl. Cryst.* **39**, 109–111.
Shimizu-Ibuka, A., Morita, Y., Terada, T., Asakura, T., Nakajima, K., Iwata, S., Misaka, T., Sorimachi, H., Arai, S. & Abe, K. (2006). *J. Mol. Biol.* **359**, 148–158.
Shirasuka, Y., Nakajima, K., Asakura, T., Yamashita, H., Yamamoto, A., Hata, S., Nagata, S., Abo, M., Sorimachi, H. & Abe, K. (2004). *Biosci. Biotechnol. Biochem.* **68**, 1403–1407.
Suzuki, M., Kurimoto, E., Nirasawa, S., Masuda, Y., Hori, K., Kurihara, Y., Shimba, N., Kawai, M., Suzuki, E. & Kato, K. (2004). *FEBS Lett.* **573**, 135–138.
Temussi, P. A. (2002). *FEBS Lett.* **526**, 1–4.
Vagin, A. & Teplyakov, A. (2010). *Acta Cryst.* D**66**, 22–25.
Walters, D. E., Cragin, T., Jin, Z., Rumbley, J. N. & Hellekant, G. (2009). *Chem. Senses*, **34**, 679–683.
Wel, H. van der (1972). *FEBS Lett.* **21**, 88–90.
Wel, H. van der, Larson, G., Hladik, A., Hladik, C., Hellekant, G. & Glaser, D. (1989). *Chem. Senses*, **14**, 75–79.
Wel, H. van der & Loeve, K. (1972). *Eur. J. Biochem.* **31**, 221–225.
Winn, M. D., Murshudov, G. N. & Papiz, M. Z. (2003). *Methods Enzymol.* **374**, 300–321.
Winn, M. D. *et al.* (2011). *Acta Cryst.* D**67**, 235–242.
Yamashita, H., Theerasilp, S., Aiuchi, T., Nakaya, K., Nakamura, Y. & Kurihara, Y. (1990). *J. Biol. Chem.* **265**, 15770–15775.
Yoon, S.-Y., Kong, J.-N. & Jo, D.-H. (2011). *Food Chem.* **129**, 1327–1330.
Zhao, G. Q., Zhang, Y., Hoon, M. A., Chandrashekar, J., Erlenbach, I., Ryba, N. J. P. & Zuker, C. S. (2003). *Cell*, **115**, 255–266.